Experimental Thermal and Fluid Science 58 (2014) 216–223

Contents lists available at ScienceDirect

Experimental Thermal and Fluid Science

journal homepage: www.elsevier.com/locate/etfs

Experimental characterization of hydraulic jump caused by jet impingement on micro-patterned surfaces exhibiting ribs and cavities

M. Johnson, D. Maynes, J. Crockett *

Department of Mechanical Engineering, Brigham Young University, Provo, UT 84602, USA

ARTICLE INFO

Article history:
Received 5 December 2013
Received in revised form 23 June 2014
Accepted 1 July 2014
Available online 23 July 2014

Keywords:
Superhydrophobic
Hydraulic jump
Slip flow
Jet impingement

ABSTRACT

This paper reports experimental results characterizing hydraulic jumps that form due to liquid jet impingement on patterned surfaces with alternating microscale-ribs and cavities. The surfaces are tested in both hydrophilic (wetted cavity regions, Wenzel state) and superhydrophobic (unwetted cavity regions, Cassie–Baxter state) states. Similar to jet impingement on a smooth surface, when a liquid jet strikes a ribbed surface it moves radially outward in a thin film and eventually experiences a hydraulic jump, where the thickness of the film increases by an order of magnitude, and the velocity decreases accordingly. However, the anisotropy of the patterned surface causes a disparity in frictional resistance resulting in a hydraulic jump which is elliptical rather than circular in shape. Both the major and minor axes radii of the hydraulic jump are a function of the jet Reynolds number and imposed downstream water depth. We obtain results for cavity fractions (relative width of cavity to total rib/cavity spacing) of 0.5, 0.8, and 0.93 and compare these to results obtained on a smooth surface. The jet issued from a nozzle with a radius of 0.6 mm, the Reynolds number ranged from 1.2×10^4 to 2.1×10^4, and a range of downstream depths were explored. The parameter ranges explored result in small scale hydraulic jumps, where the jump radii are generally smaller than a few centimeters. Results show both major and minor axis jump radii decrease with increasing water depth or decreasing jet Reynolds number, following classical hydraulic jump behavior. When the Wenzel state exists, the major axis is nominally the same for both the smooth and structured surfaces at the same Reynolds number and downstream depth. For both the Wenzel and Cassie–Baxter states, as the cavity fraction of the superhydrophobic surface increases, the major axis of the hydraulic jump radius increases modestly and the minor axis decreases. These changes are exaggerated when the Cassie–Baxter state prevails. Also, as the cavity fraction increases the eccentricity of the jump increases, and this is more pronounced when the Cassie–Baxter state exists.

1. Introduction

The focus of this paper is the dynamics of a small-scale liquid jet interacting with a surface that is structured with microscale patterning where the surface may be either hydrophilic or superhydrophobic. When a vertical liquid jet strikes a smooth horizontal surface, the liquid subsequently spreads radially in a circular thin film until a hydraulic jump occurs, which is characterized by a sudden large increase in liquid depth and corresponding decrease in the average velocity of the fluid. This is illustrated in the top panel of Fig. 1 and described by Watson in his seminal paper [1]. Watson developed a model of the thin film and resulting hydraulic jump based on conservation of mass and momentum which accounted for the boundary layer in the thin film region and thus the viscous influences throughout this region [1]. Many experimental studies have been performed and compared to Watson's analysis, with varying agreement dependent on flow dynamics within the jump. Experiments have found various jump shapes and flow structures immediately downstream of the jump [2–9]. Liu and Lienhard [6] observed that while Watson's model is generally accurate for jumps of large radii, it over predicts the jump radius for jumps of small radii. In this case surface tension becomes significant and reduces the diameter of the jet. Bush and Aristoff updated Watson's laminar model to account for the surface tension force caused by curvature of the free surface at the jump location [7]. This reduced the shortcoming in Watson's original model when the imposed downstream depth, H, is large and the jump radius, R_j, is small and resulted in better agreement with experimental data.

While a general understanding of jet impingement on uniform smooth surfaces has been explored, impingement on microscale

* Corresponding author.
E-mail address: crockettj@byu.edu (J. Crockett).

http://dx.doi.org/10.1016/j.expthermflusci.2014.07.001
0894-1777/

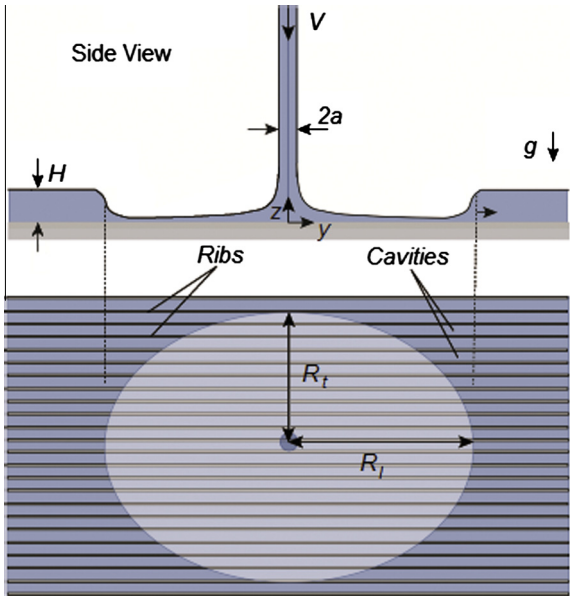

Fig. 1. Schematic illustration of liquid jet impingement on a SH surface with the top panel showing the side view and the bottom panel showing a top view. Rib patterning is not to scale, hundreds to thousands of rib-and-cavity features are covered by the thin film.

or nanoscale structured surfaces is less well understood and experimental characterization of the hydraulic jump that forms on such surfaces is the focus of this work. In particular, this paper addresses small scale hydraulic jumps of nominal diameter smaller than a few centimeters. The dynamics of the flowing thin film and location of the hydraulic jump are dependent on the surface patterning and whether the surface material is natively hydrophilic (i.e. uncoated pure silicon) and water floods the cavities (Wenzel state) or the surface material is coated with a hydrophobic coating causing the water to sit above the cavities, resulting in a vapor–liquid interface over the majority of the surface (Cassie–Baxter state) which is deemed superhydrophobic. At this vapor–liquid interface an apparent slip is present [10], which when averaged over the surface increases as the relative size of the cavity regions increases [11,12]. The apparent slip of the surface may be defined in terms of a slip length, λ, which represents the wall-normal distance, into the wall, where the velocity of the fluid would vanish, and is a function of the wall structuring characteristics and hydrophobic coating. As λ increases, the shear at the surface decreases, and the apparent velocity at the surface increases.

Some recent studies explore the influence of variations in surface topology on the thin-film flow physics and associated hydraulic jump transitions as a result of jet impingement on the surface [13–17]. Dressaire et al. [13,14] created surfaces with micro-post arrays, immersed them in the Wenzel state and found polygonal and star shaped hydraulic jumps where the vertices were located along the path of least resistance, in between the posts. Different shapes were achieved depending on the pattern of the posts on the surface. The average jump radius compared well to the analytical model provided by Bush and Aristoff [7].

Surfaces where the liquid exists in the Cassie–Baxter state are expected to behave differently than those when the Wenzel state prevails. Maynes et al. [15] studied jet impingement on unimmersed superhydrophobic surfaces with alternating micro-scale ribs and cavities. Impingement on surfaces in the Cassie–Baxter state did not result in the classical hydraulic jump, but the thin film broke into filaments or droplets due to surface tension influences. The shape of the thin film breakup location was elliptical. Impingement on surfaces in the Wenzel state also yielded an elliptical hydraulic jump. However, the downstream depth was neither imposed nor measured, therefore the hydraulic jump measurements could not be compared to findings from previous experimental studies or analytical solutions.

No previous experiments have been conducted that characterize the hydraulic jump due to jet impingement on a micro-patterned surface, in either the Cassie–Baxter or Wenzel state, with a maintained downstream depth. This paper reports results in this unexplored area with micro-patterned surfaces exhibiting alternating micro-ribs and cavities as can be seen in the bottom panel of Fig. 1. Note the rib-and-cavity features in Fig. 1 are not to scale. Surfaces with microscale ribs and cavities yield a significant difference in frictional resistance in both the Wenzel and Cassie–Baxter states between the flow directions parallel and perpendicular to the ribs. The focus of the work is an experimental characterization of jet impingement and the resultant hydraulic jump location on surfaces with anisotropic rib/cavity structuring. Results when both the Wenzel and Cassie–Baxter states prevail are explored and compared over a range of experimental conditions spanning the range of laminar jet impingement dynamics. Section 2 describes the experimental methods of the research, in Section 3 the results are discussed, and in Section 4 we provide conclusions of the work.

2. Experimental method

Test surfaces were fabricated from silicon wafers 101.6 mm in diameter using standard photolithographic processes. Since silicon is natively hydrophilic, uncoated patterned surfaces were used to explore the behavior when the surfaces were in the Wenzel state. To achieve the Cassie–Baxter state, the silicon surfaces were coated with a thin layer of chromium, for adhesion purposes, and then Teflon. Rib and cavity surface structures were created where the width of a cavity is defined as w_c, the total width of a rib and cavity is defined as w, and the cavity fraction is the ratio of these quantities, $F_c = w_c/w$. Three surface patterns were employed with cavity fractions of $F_c = 0.5$, 0.8, and 0.93. Scanning electron microscope (SEM) images of the surfaces used are shown in Fig. 2. The rib height was nominally 15 μm, for each surface. The total width of a rib and cavity is $w = 40$ μm for all surfaces. This cavity width ensures that for coated surfaces the Laplace pressure due to the surface tension [18] will not be exceeded, except in the jet stagnation region, and the Cassie–Baxter state will prevail. Polished silicon wafers were used for the smooth surfaces ($F_c = 0$). Six jet velocities were explored for each surface, yielding a jet Weber number range of $We = \rho V^2 a/\sigma = 3 \times 10^2 - 1 \times 10^3$ and corresponding Reynolds number range of $Re = Q/av = 1.2 \times 10^4 - 2.1 \times 10^4$, where V is the jet velocity, a is the jet radius, ρ is the fluid density, σ is the surface tension, v is the fluid kinematic viscosity, and Q is the volume flow rate. Note the jet Reynolds number used here is related to the internal pipe flow Reynolds number through $Re_{pipe} = 2Re/\pi$, such that the range of pipe Reynolds numbers is $Re = 7.6 \times 10^3 - 1.3 \times 10^4$. No surface instabilities were visually observed with respect to the jet, although turbulence intensity within the jet dampens rapidly upon impingement due to the strong adverse pressure gradient associated with stagnation, somewhat laminarizing the flow in the thin-film region [19,20]. The radial jump locations in the longitudinal and transverse directions are presented for the above surfaces and Reynolds numbers, and for imposed normalized downstream depths ($\widehat{H} = H/a$) ranging from 5 to 12.5.

The test apparatus consists of a vertically oriented nozzle of radius $a = 0.6$ mm located 20 mm above the horizontal test surface of interest, shown in Fig. 3. The nozzle was fed by a plenum filled with deionized water with an adjustable pressure to achieve the desired flow rate. The surface tension was determined from published information based on temperature measurements of the